Structure-Composition Relationships in Ternary Solvents Containing Methylbenzoate

S. Aparicio, R. Alcalde, B. García, and J. M. Leal*

Departamento de Química, Universidad de Burgos, 09001 Burgos, Spain

Received: August 31, 2007; In Final Form: December 18, 2007

Thermophysical properties of the hexane + 1-chlorohexane (or hexanoic acid or diisopropylether) + methylbenzoate ternary systems and their binary constituents are reported at 298.15 K and 0.1 MPa over the whole composition range. The properties and the optimized geometry of the gas-phase components were appraised from the density functional theory. To find out the causal link between the thermophysical measurements and the molecular level features, the derived mixing and excess functions of the ternary systems were looked into according to the scaled particle and Kirkwood−Buff analyses. The hydrogen bonding and dipole interactions along with the geometry effects brought about by the very different size and shape of the components give rise to complex mixed structures. Application of semiempirical models and use of simple cubic equations of state combined with a one-parameter van der Waals mixing rule has led to prediction of the ternary properties with variable degree of precision.

Introduction

An appropriate choice of multicomponent solvent media bears a considerable importance for the efficiency of large-scale processes.[1,2] Environment regulations have speeded up the use of green solvents with low toxicity and improved recycling ability; however, the involvement of suitable solvent formulations in process designs requires knowledge of accurate thermophysical properties of solvent mixtures,[3,4] which often constitutes a technological challenge.[5,6] Although the most reputable way of dealing with this objective is a precise measure of such properties, in practice the large number of possible combinations makes measurements over wide temperature and pressure ranges unfeasible.[7] In particular, the lack of information on multicomponent mixtures has prompted the development of models that may predict properties of ternary mixtures from the binary constituents.

The molecular fluid structure determines the macroscopic properties; however, the carrying out of convincing predictions would require such a detailed knowledge of the structure and intermolecular forces that often is unavailable.[8,9] It is not always easy to discern which microscopic property is the source for an observed macroscopic magnitude; hence, although certain molecular information can be drawn from macroscopic measurements, the experimental data must be addressed carefully. Conclusions on fluid structures drawn far from a grounded basis may lead to erroneous interpretations. Therefore, to overcome this mismatch the use of statistical mechanics is desirable, and the study of properties of liquid mixtures should aim at two ends: (i) obtaining comprehensive sets of data for testing theoretical models,[10,11] and (ii) the use of sound statistical mechanic approaches to derive tried and true molecular analyses from macroscopic properties.[12,13]

Methylbenzoate (MB) is an important aromatic ester widely used as a solvent. Aromatic esters are aprotic solvents interesting for many settings. The hydrophobic nature and the polarizable π-electron system close to the dipolar ester site confer a beneficial selective ability in synthesis, cosmetic formulations, and polymer science. However, despite their recognized importance, so far only few systematic studies on mixtures containing aromatic esters have been reported.[14] This work is aimed at contributing to a better understanding of MB-containing mixtures giving away the facts that govern their behavior.[15] The thermophysical properties of the hexane (HEX) + 1-chlorohexane (Cl-HEX) [or hexanoic acid (HEX-Ac) or diisopropylether (DIPE)] + MB ternary systems were looked into at 298.15 K and 0.1 MPa over the whole composition range. To perform a wider study that takes in the effect of different groups, the second component was chosen by marrying up six carbon atoms (hexane, the first and common component) with three relevant groups; this combination may provide a useful structure/composition relationship and contribute to shed light to the mixture structure.

In this work, several models have been put forward to settle the linkage between the structural information at molecular level and the experimental measurements. A further critical analysis comes from the scaled particle (SP)[16] and the Kirkwood−Buff (KB)[13] methods in the inverted version by Ben−Naim.[17] Both approaches were used to interpret the intermolecular interactions, the steric effects, and the preferential solvation of the studied mixtures. The ternary properties were predicted, on one hand, using simple semiempirical models[18] and, on the other hand, according to the Soave−Redlich−Kwong (SRK)[19] and Peng−Robinson (PR)[20] equations of state (EOS) combined with a one-parameter van der Waals-type mixing rule. Because of their simplicity and relative reliability, these EOS are widely used for process design.[21]

Materials and Methods

The solvents HEX (99.5%), Cl-HEX (99.5%), HEX-Ac (99.6%), DIPE (99.2%), and MB (99.9%) were obtained from various sources and used without further purification. The liquids, fully miscible over the whole composition range, were degassed with ultrasound and kept out of the light over Fluka Union Carbide 0.4 nm molecular sieves. Their purity was

* Corresponding author. E-mail: jmleal@ubu.es.

10.1021/jp076996i CCC: $40.75
Published on Web 02/23/2008

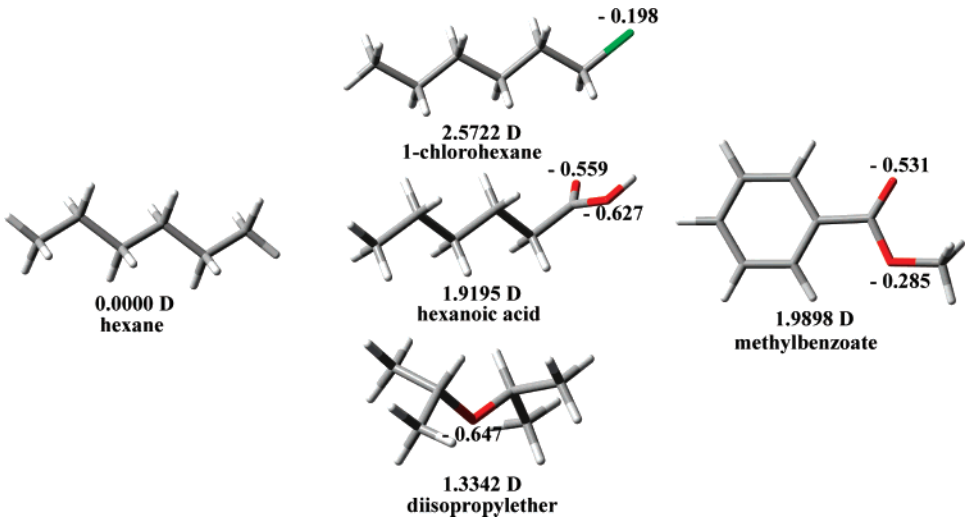

Figure 1. Structure, dipole moment, and MK charges (only for oxygen and chlorine atoms) of the gas-phase monomers optimized at B3LYP/6-311++g** theoretical level. Color code: (dark gray) carbon, (light gray) hydrogen, (red) oxygen, and (green) chlorine.

assessed by gas chromatography with a Perkin-Elmer 900 apparatus and by comparing the measured properties with available literature data (Table S1, Supporting Information). The samples were prevented from preferential evaporation by syringing amounts of the cooled liquids, weighed to $\pm 10^{-5}$ g with a Mettler AT261 balance, into suitably stoppered bottles with a stated $\pm 10^{-4}$ precision in mole fraction. To ensure a fair description of the ternary mixtures, the samples were evenly distributed over the whole composition scale following the procedure previously reported.[26]

The density readings, ρ, based on the mechanical oscillator measuring principle, were measured with a computer-controlled DMA 58 Anton Paar digital density Meter ($\pm 5 \times 10^{-6}$ g cm^{-3}) equipped with a Peltier element that ensures thermostatization to ± 0.01 K. Proper calibration was achieved at all working temperatures with deionized doubly distilled water (Milli-Q, Millipore) and *n*-nonane (Fluka, 99.2% GC) as reference liquids; the density values for these standards were obtained from the NIST webbook.[27] Dynamic viscosities, η, were measured with an automated AMV 200 Anton Paar microviscometer. The viscosity measurements are based on the rolling ball measuring principle: a gold-covered steel ball is introduced into an inclined, sample-filled, thermostatted (± 0.005 K) glass capillary. The time (± 0.01 s) needed for the ball to roll a fixed distance between two magnetic sensors is turned into viscosity readings (± 0.005 mPa s). The calibration constants at every inclination angle and working temperature were evaluated using doubly distilled water as a reference.[27] Readings for both properties, ρ and η, were taken concurrently using an Anton Paar SPV sample changer with a peristaltic pump. Refractive indices, n_D, were measured ($\pm 5 \times 10^{-5}$) using the sodium *D* line of an automatic Leica AR600 thermostatted refractometer (± 0.01 K) and the apparatus was calibrated using water[22] and a reference oil ($n_D = 1.51416$) as standards. A prism equipped with a lid produces tightness and preserves the sample from preferential evaporation.

Results and Discussion

Density Functional Theory (DFT) Calculations. An ab initio study of the thermophysical properties of the components may provide a structural knowledge of the mixtures. Full gas-phase optimization of the molecules involved was carried out using DFT with the three-parameter Becke gradient-corrected exchange functional[28] in conjunction with the Lee−Yang−Parr correlation functional (B3LYP).[29,30] The electrons far from and close to the nuclei were described using large and flexible basis sets, here, the 6-311++g** basis set. To reliably fit the electrostatic potential,[31] the respective atomic charges were calculated according to the Merz−Singh−Kollman (MK)[32] scheme; the fitting procedure was constrained to reproduce the overall molecular dipole moment. The charges calculated with the MK scheme showed only a soft variation with the computational method and the basis set employed; hence, these can be regarded as superior to Mulliken charges. The calculations were performed with *Gaussian 03*.[33]

Figure 1 shows the gas-phase optimized structures, dipole moments, and MK charges of the components. Although the molecular properties may certainly vary from gas to liquid phase, to fairly analyze the observed effects in liquid mixtures several conclusions drawn from the gas phase study may be saved. On the other side, given the multicomponent nature of the studied mixtures, simulation of the molecular properties in solution would require knowledge of the property change with the mixture composition, which exceeds the scope of this work; relevant molecular properties such as size and shape, quite useful to study the liquid mixture behavior, may be inferred from gas-phase computations.

The HEX linear structure gives rise to a null dipole moment;[34] therefore, the main contribution to the mixture structure consists of either dispersive forces and/or the steric effects arising from the linear shape and the molecular rotational flexibility. The Cl-HEX linear structure, with a high dipole moment due to the Cl atom effect (Figure 1), results in strong dipole interactions and shape effects. The HEX-Ac structure, characterized mainly by the carboxyl group, bears strong negative charges located at the two oxygen atoms (larger for the OH oxygen) and a noticeable dipole moment; moreover, the H-bonding ability of carboxylic acids and the structural effects brought about by its linear shape is well known. In contrast, DIPE affects the mixture's properties overall by its size and shape; in fact, the large negative charge on the ether oxygen, which yields only a modest dipole moment, is partially hidden in the spherical shape molecular framework, and interaction through this site is hindered. Molecules with similar globular structure often have affected the mixture structure.[15b]

Finally, calculations point to a planar structure for MB, the ring/ester zero dihedral angle leading to a significant dipole

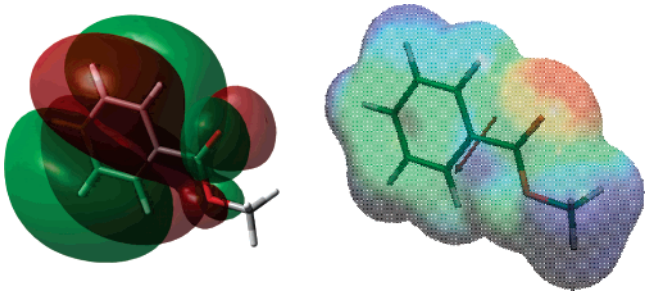

Figure 2. B3LYP/6-311++g** calculated gas phase (left) HOMO orbital (isovalue 0.002 au) and (right) ESP mapped on an electronic density surface (isovalue 0.0002 au). Color scale for ESP: (blue) positive to (red) negative. Arrow is for the molecular dipole moment.

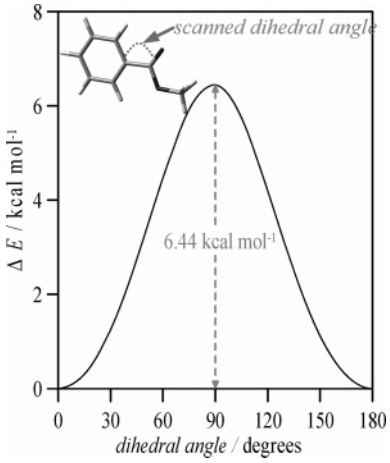

Figure 3. B3LYP/6-311++g** calculated gas-phase relaxed potential energy scanning for the showed dihedral angle in MB. ΔE is the energy relative to the minimum value.

moment with a notable charge at the C(=O) site (Figure 2). The highest occupied molecular orbital (HOMO) structure, outlined in the in-phase orbitals and borne out by the electrostatic surface potential (ESP), gives away ring-ester electrostatic interaction through the C(−O−)CH_3 site. Figure 2 also shows the negative ESP surrounding the nucleophilic CO oxygen (which arises from the MK negative electrostatic charge); hence, electrostatic interactions through such nonsterically hindered sites is feasible. The effective ring-ester interaction through this site brings about the MB planar shape. Likewise, the moderate ring-ester torsional barrier (Figure 3) is in favor of such a planar shape. The calculated gas-phase IR spectrum (Figure 4) shows intense vibration peaks of the MB ester group, and out-of-plane (oop) those of the aromatic ring; hence, the planar shape arising from the more effective interaction between both groups determines the MB properties.

Some Remarks on Excess and Mixing Properties. Tables S2 and S3 (Supporting Information) list the (novel) measured properties for the ternary systems and their binary constituents; properties for the remaining binary mixtures may be found in previous works.[15a,b] Molar excess volume (V_m^E), mixing viscosity ($\Delta_{mix}\eta$), and mixing refractive index ($\Delta_{mix}n_D$) were evaluated from the experimental readings according to the expressions reported earlier.[15] Excess thermodynamic properties reflect the nonideal behavior of mixtures and can be attributed to (a) the difference in shape and size between components, (b) the difference between like−like and unlike interactions, and (c) the molecular reorientation in the mixture. Although the interpretation of parameters such as $\Delta_{mix}\eta$ and $\Delta_{mix}n_D$ is not a straightforward one, these mixing properties bear relation

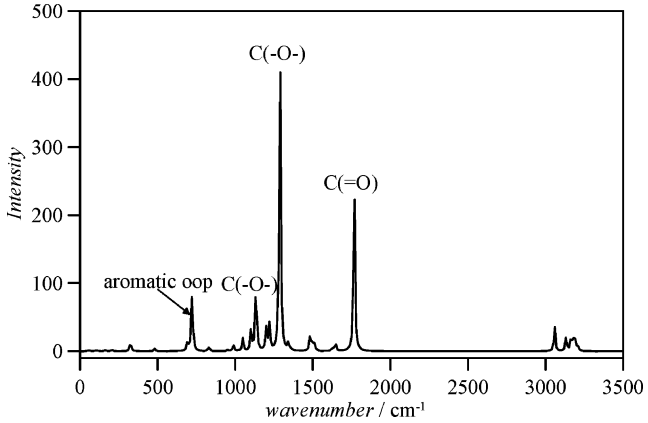

Figure 4. B3LYP/6-311++g** calculated gas-phase IR spectrum of MB.

with the fluid structure. The excess and mixing properties for the binary constituents, X^E, were correlated with composition, x, using the Redlich−Kister equation[35]

$$X^E = x(1-x)\sum_{j=1}^{k} A_j(2x-1) \qquad (1)$$

with the A_j coefficients being obtained by a least-squares procedure and the proper number of coefficients, k, and standard deviations determined by an F-test (Table S4, Supporting Information). The ternary excess and mixing properties, X_{TER}^E, were fitted to Cibulka equation[36]

$$X_{TER}^E = X_{BIN}^E + x_1x_2x_3(B_0 + B_1x_1 + B_2x_2) \qquad (2)$$

where X_{BIN}^E stands for the sum of the particular property for the three binary constituents deduced with eq 1 using the parameters of Table S4 (Supporting Information) and those previously reported.[15a,b] The last term in eq 2 is the so-called ternary contribution to the corresponding property; the parameters deduced from a least-squares procedure are listed in Table S5 (Supporting Information), and the maxima and/or minima of the resulting ternary contributions in Table S6 (Supporting Information).

Partial molar quantities, defined as the rate of change with concentration of extensive functions, account for the binary and higher order interactions between components. From the fitting coefficients of molar excess volumes (Tables S4 and S5, Supporting Information), the partial molar excess properties, $\bar{V}_m^E$, were evaluated for both the ternary systems and their binary constituents according to the intercept method;[15] the limiting values at infinite dilution were evaluated as the values at mole fraction approaching zero. The high quality of the fitting functions used to describe molar excess volumes assures the feasibility of the derived partial molar properties. Plots of the excess and mixing properties for the ternary and binary mixtures are given in Figures 5−12; for an easier view of the ternary behavior, projections of the leveling curves for the three-dimensional plots are also provided.

Thermophysical Properties of the Binary Constituents. The properties of HEX + MB, and Cl-HEX (or HEX-Ac or DIPE) + MB binary constituents were reported earlier,[15a,b] whereas the required data for HEX + Cl-HEX (or HEX-Ac or DIPE) are reported in Table S2 (Supporting Information) and plotted in Figures 5 and 6; the properties and structure of the binary constituents are strongly affected, on one side, by the

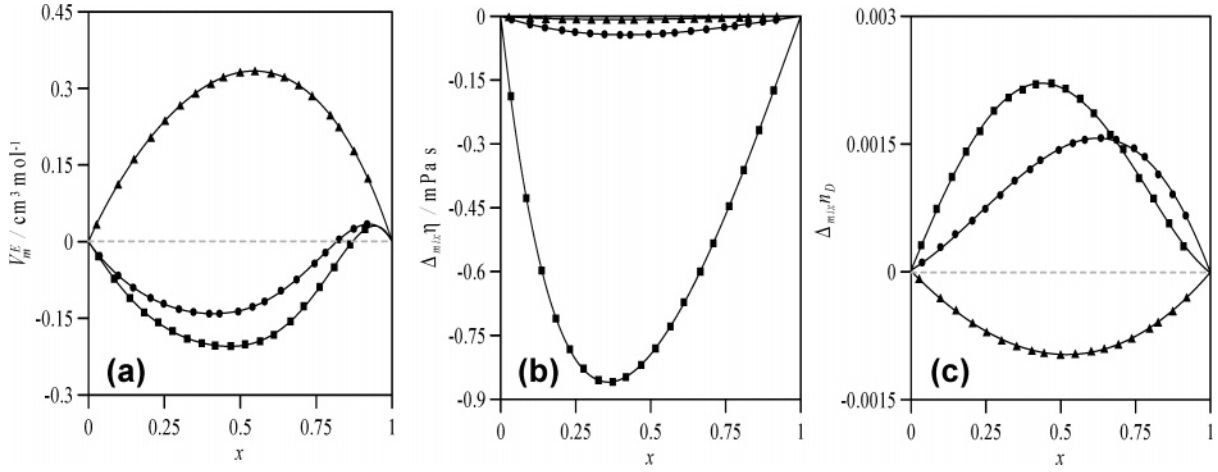

Figure 5. (a) Molar excess volume, V_m^E, (b) mixing viscosity, $\Delta_{mix}\eta$, and (c) mixing refractive index, $\Delta_{mix}n_D$, for the x HEX + $(1 - x)$ {(●) Cl-HEX or (■) HEX-ac or (▲) DIPE} binary systems at 298.15 K and 0.1 MPa.

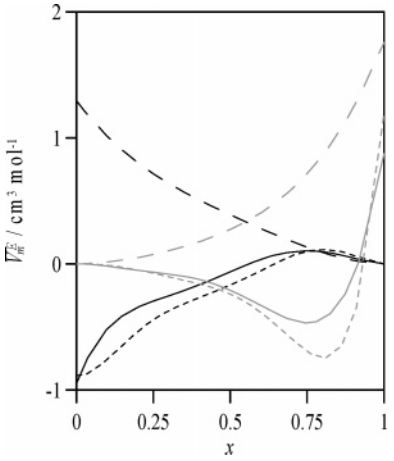

Figure 6. Partial molar excess volume, $\bar{V}_m^E$, of HEX (black lines) and cosolvent (gray lines) for the x HEX + $(1 - x)$ {(—) Cl-HEX or (---) HEX-Ac or (− −) DIPE} binary systems at 298.15 K and 0.1 MPa. Values calculated from parameters reported in Table S4 (Supporting Information).

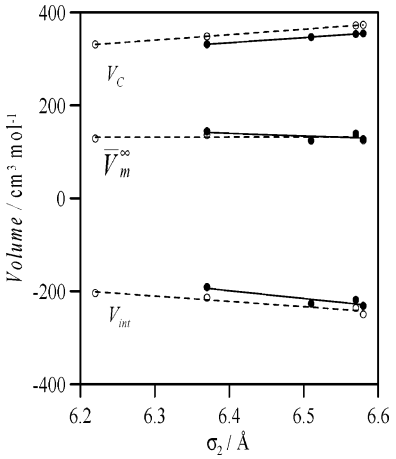

Figure 7. Cavity, V_c, interaction, V_{int}, and partial molar volume at infinite dilution, $\bar{V}_m^\infty$, volumes for different binary mixtures as a function of solute hard sphere radii, σ_2. Data from Table 2. (—,●) solvent, HEX; (---, ○) solvent, MB. Linear fits included to show trends. From lower to higher σ_2 (from left to right in the plot): HEX, DIPE, MB, Cl-HEX, and HEX-Ac.

size and shape of the components and, on the other, by dipolar forces and specific interactions like those in HEX-Ac-containing mixtures.

The MB-containing mixtures are prone to disruption of the ester structure upon addition of a second component; however, despite the difference in shape between components, the negative molar excess volumes reveal the mutual fair fitting between components that produces an efficient packing, even with the spherical-like DIPE.[15a,b] Such a cosolvent accommodation would in principle favor a closer approach between components. The observed negative mixing viscosity, on one side, reflects absence of strong specific forces, such as MB/HEX-Ac H-bonding and, on the other side, points to weak dipolar forces among mixture molecules. These, however, do not make up for the disruption of dipolar ordering in pure fluids upon mixing; hence, geometrical effects appear to be the main controling factor of the mixture structure.

Among all HEX-containing binary mixtures investigated, the properties of the DIPE system stand out. The sharply different DIPE and HEX shapes hampers the mutual packing, giving rise to a pronounced expansive trend (Figure 5a) even at high dilution (Figure 6); the positive partial molar excess volumes in HEX + DIPE mixtures (Figure 6) disclose the mutual hindered packing over the whole composition range. Despite being the only HEX-containing system with positive excess volume, this system with DIPE shows the lowest negative and close to zero mixing viscosity. This feature can be justified considering that the difficult HEX/DIPE packing also hinders the mixture fluidity and thus the almost null mixing viscosity despite the clear expansion upon mixing.

Cl-HEX and HEX-Ac-containing mixtures yielded a more efficient packing; their almost linear size and shape, similar to that of HEX, give rise to negative molar excess volumes. Only at very low cosolvent concentration slightly positive values have emerged, which also give rise to positive partial molar excess volumes (Figure 6). The Cl-HEX binary system shows a slightly negative mixing viscosity, showing that the disruption effect of HEX on the Cl-HEX dipolar ordering is not very strong. Anyway, the slightly positive excess volume in rich HEX regions shows the breaking effect of the Cl group on the HEX-dominated structure.

Although the volumetric behavior of HEX-Ac-containing mixtures resembles that of Cl-HEX, the remarkably negative mixing viscosity values for HEX-Ac clearly differ. In fact, pure HEX-Ac behaves as a mixture of polar monomers dispersed in a dominated medium consisting of apolar cyclic H-bonding dimers (Figure 1);[37] addition of HEX to such an acid-dominated structure hinders the dimer formation, thus boosting the

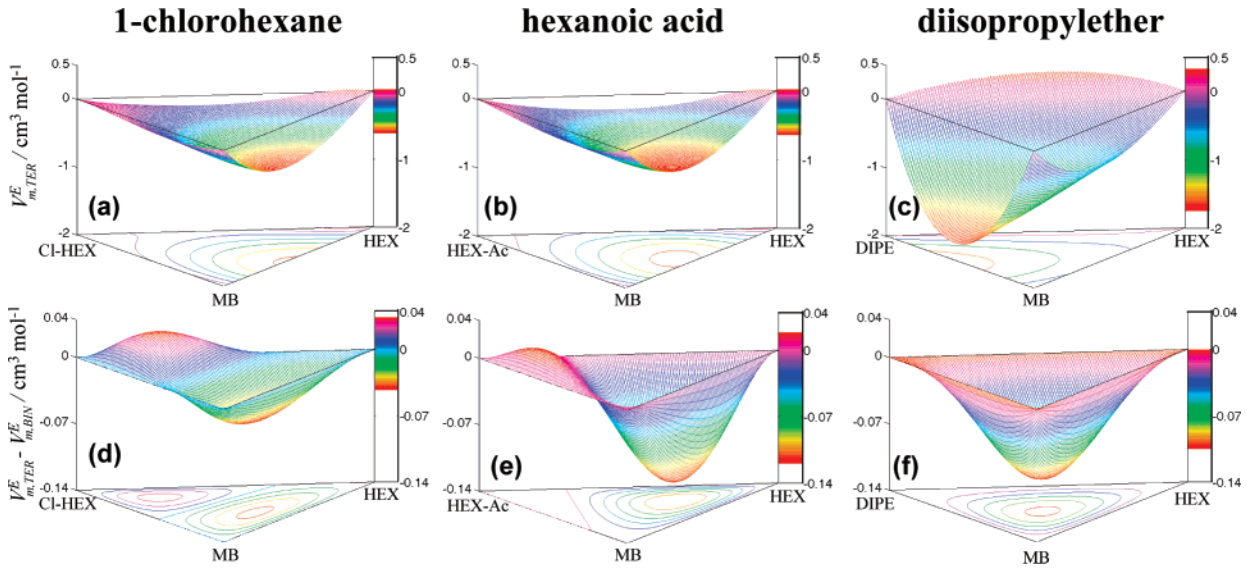

Figure 8. Molar excess volume, $V^{E}_{m,TER}$, and ternary contribution to molar excess volume, $V^{E}_{m,TER} - V^{E}_{m,BIN}$, for the x_1 HEX + x_2 Cl-HEX (or HEX-Ac or DIPE) + $(1 - x_1 - x_2)$ MB ternary systems at 298.15 K and 0.1 MPa. Figure heading for the second mixture component.

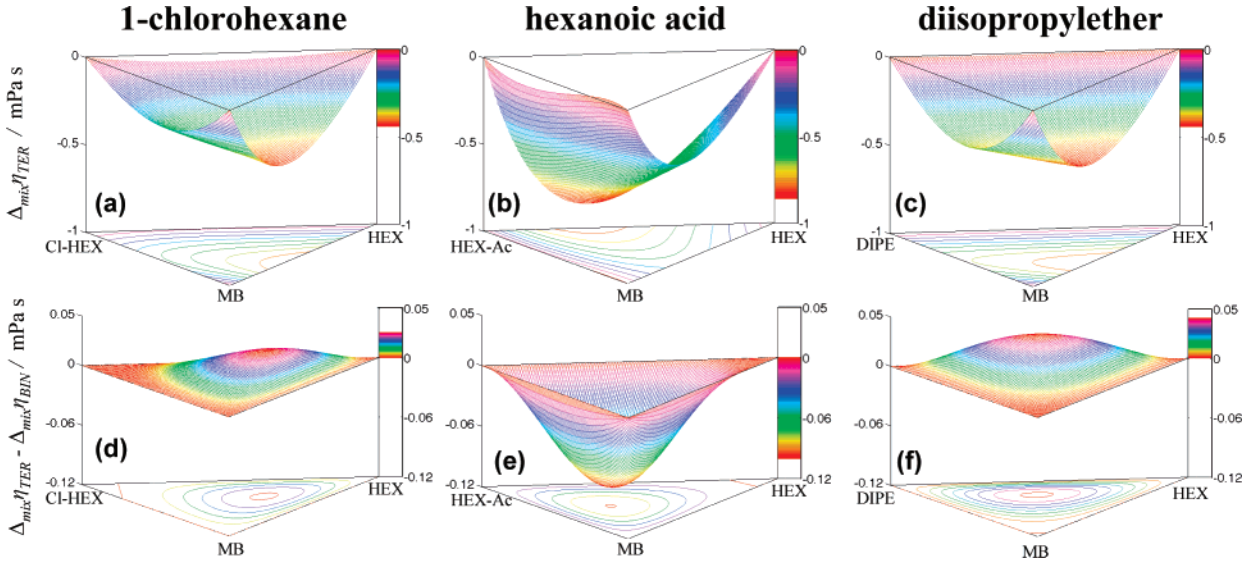

Figure 9. Mixing viscosity, $\Delta_{mix}\eta_{TER}$, and ternary contribution of mixing viscosity, $\Delta_{mix}\eta_{TER} - \Delta_{mix}\eta_{TER}$, for the x_1 HEX + x_2 Cl-HEX (or HEX-ac or DIPE) + $(1 - x_1 - x_2)$ MB ternary systems at 298.15 K and 0.1 MPa. Figure headings for the second mixture component.

monomer population, which better fit onto the HEX molecules and give rise to a remarkably lower viscosity.

The derived property partial molar volume at infinite dilution, $\bar{V}^{E,\infty}_{m}$measures the solute−solvent forces and involves geometry effects and intermolecular interactions. In addition to the intrinsic solute volume, solute−solvent forces are the main factor that govern the solvent packing around a central solute unit. Therefore, an analysis of the $\bar{V}^{E,\infty}_{m}$ values lends an insight into the mixture structure; this can be carried out straightforward with the SP theory,[16] which splits the $\bar{V}^{E,\infty}_{m}$ values into different contributions in the form

$$\bar{V}^{E,\infty}_{m,i} = V_c + V_{int} + k_T RT - V_i \qquad (3)$$

where V_c and V_{int} stand for the cavity formation and solute−solvent interaction contributions, respectively. According to the SP model, the transfer of a solute from a gas to a liquid can be conceived in two steps: (i) formation of a suitably sized solvent cavity capable of hosting the solute molecule with the result of the V_c expansion, and (ii) introduction of solute molecules into the solvent cavities, which results in the V_{int} solute−solvent interaction contraction term. From a molecular standpoint, the V_c values corresponding to partial molar volumes of a hypothetical noninteracting spherical molecule can be calculated as

$$V_c = \frac{4}{3}\pi N_A\left(\frac{\sigma_2}{2}\right)^3 + k_{T,1}RTy(1-y)^{-3}\left((1-y)^2 + \frac{3(1-y)\sigma_2}{\sigma_1} + 3(1+2y)\left(\frac{\sigma_2}{\sigma_1}\right)^2\right) \qquad (4)$$

$$y = \frac{\pi N_A {\sigma_1}^3}{6V_1} \qquad (5)$$

where subscripts 1 and 2 refer to solvent and solute, respectively, and σ_i represents the hard-sphere radii calculated from vaporization enthalpies. V_{int} is calculated from the experimental $\bar{V}^{E,\infty}_{m}$ and V_c values obtained from eqs 4 and 5. The component properties required for SP calculations are listed in Table 1.[38−43] The rather similar hard-sphere radii of the molecules involved point to strong geometry effects on mixing with a notable

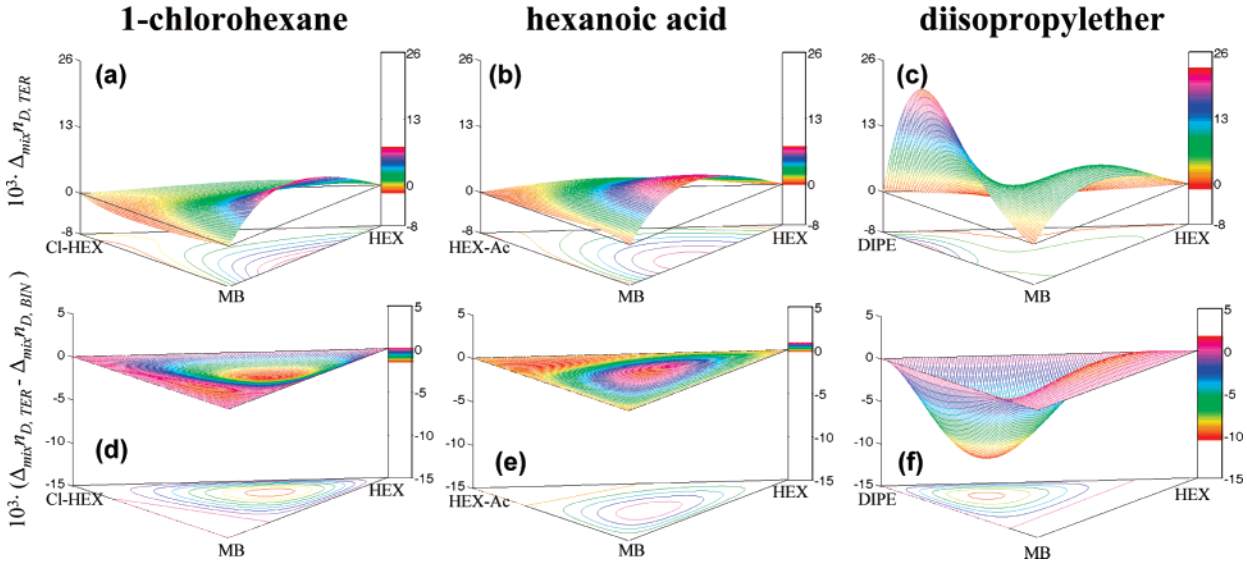

Figure 10. Mixing refractive index, $\Delta_{mix}n_{D,TER}$, and ternary contribution of mixing refractive index, $\Delta_{mix}n_{D,TER} - \Delta_{mix}n_{D,BIN}$, for the x_1 HEX + x_2 Cl-HEX (or HEX-Ac or DIPE) + $(1 - x_1 - x_2)$ MB ternary systems at 298.15 K and 0.1 MPa. Figure headings for the second mixture component.

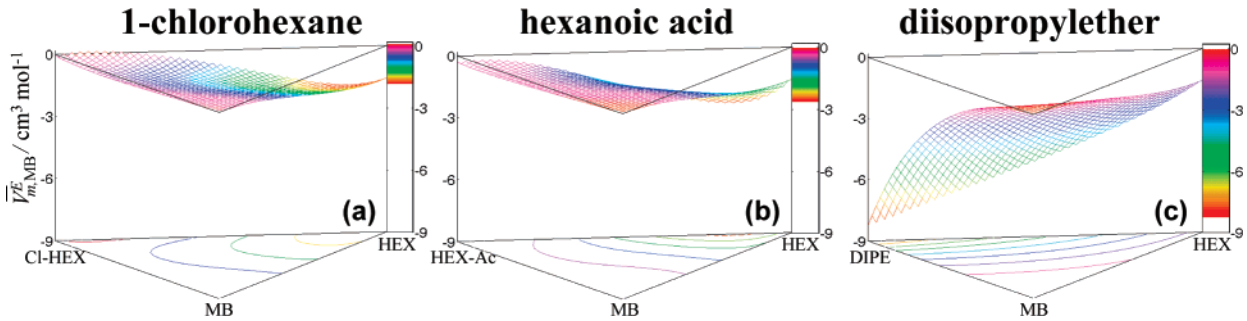

Figure 11. Partial molar excess volume of MB, $\bar{V}^{E}_{m,MB}$, in the x_1 HEX + x_2 (Cl-HEX or HEX-Ac or DIPE) + $(1 - x_1 - x_2)$ MB ternary systems at 298.15 K and 0.1 MPa. Figure headings for the second mixture component.

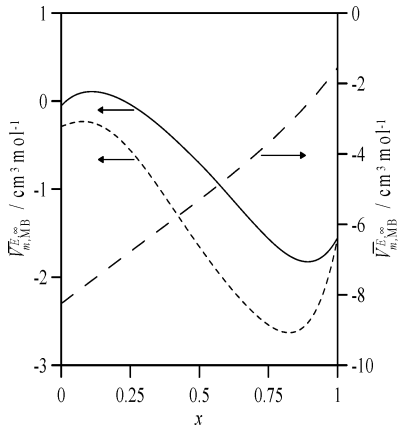

Figure 12. MB infinite dilution partial molar excess volume, $\bar{V}^{E,\infty}_{mix,MB}$, for the x_1 HEX + x_2 Cl-HEX (or HEX-Ac or DIPE) + $(1 - x_1 - x_2)$ MB ternary systems at 298.15 K and 0.1 MPa. $\bar{V}^{E,\infty}_{mix,MB}$ as a function of x HEX + $(1 - x)$ {(—) Cl-HEX or (---) HEX-Ac or (— —) DIPE} with $x_{MB} \rightarrow 0$.

disruption. The size of the mixed molecules would favor an efficient packing; hence, addition of a solute to a fluid dominated by a second component of similar size would allow an efficient fitting of the solute into the solvent structure and, thus, a disruption of the forces present in the solvent structure. For DIPE, not only the molecular size must be taken into consideration, but also the shape, which hinders the packing in a fluid dominated by almost linear molecules. The SP results deduced (Table 2) show large positive V_c values for the binary

TABLE 1: Isobaric Thermal Expansivity, α_p, Isothermal Compressibility, k_T, Molar Volume, V, van der Waals Volume, V_W, Standard Vaporization Enthalpy, ΔH^o_V, and Hard−Sphere Diameter, σ, at 298.15 K

component	α_p/ k K^{-1}	k_T/ T Pa^{-1}	V/ $cm^3\,mol^{-1}$	V_W/ $cm^3\,mol^{-1}$	ΔH^o_V/ kJ mol^{-1}	σ/Å
MB	0.882[a]	580[e]	125.64[g]	76.24[h]	55.57[i]	6.51[k]
HEX	1.389[a]	1609[f]	131.57[g]	67.52[h]	31.55[j]	6.22[k]
Cl-HEX	1.038[b]	1019[b]	138.08[g]	75.97[h]	42.8 [j]	6.57[k]
HEX-Ac	0.921[c]	770[c]	125.99[g]	73.74[h]	73.2[i]	6.58[k]
DIPE	1.460[d]	1732[d]	142.29[g]	72.81[h]	32.12[j]	6.37[k]

[a] Ref 15a. [b] Ref 38. [c] Ref 39. [d] Ref 40. [e] Unpublished PVT results from the authors. [f] Ref 41. [g] This work. [h] Calculated according to the Group Contribution procedure reported in ref 41. [i] Ref 27. [j] Ref 43. [k] Calculated using α_p and ΔH^o_V according to the procedure by Pierotti, ref 16.

constituents (Figure 7) and somewhat lower, negative, V_{int} values. In terms of expansion, the V_c values of HEX-containing systems, lower than those with MB, reveal that solute fitting into the MB structure becomes difficult; this trend is borne out by the closer HEX size and shape to those of the solute compared to the planar MB, which to reach an efficient fitting, requires prior solute readjustment to the MB structure. As expected, the V_c values rose for both solvents as the solute hard-sphere radii increased, and the interaction volume dropped off to even more negative values as the solute radii increased. Although the values were remarkably large, this property did not fully make up for the expansion arising from the cavity formation. The V_{int} contribution was slightly more negative in

TABLE 2: SP Theory Properties: Cavity Volume, V_c, Interaction Volume, V_{int}, and y Function, and Experimental Solute Partial Molar Excess Volume at Infinite Dilution, $\bar{V}_m^{E,\infty}$, at 298.15 K for the Solutes and Mixtures Considered

solvent	solute	$\bar{V}_m^{E,\infty}$/ cm^3 mol^{-1}	V_c/ cm^3 mol^{-1}	V_{int}/ cm^3 mol^{-1}	y
HEX	MB	−1.56	346.65	−226.55	0.5764
MB	HEX	−3.17	330.93	−203.96	0.6918
HEX	Cl-HEX	0.87	353.41	−218.45	0.5764
Cl-HEX	HEX	−0.95	349.76	−221.67	0.6480
HEX	HEX-Ac	1.19	354.55	−231.36	0.5764
HEX-Ac	HEX	−0.89	507.62	−378.84	0.7141
HEX	DIPE	1.76	331.19	−191.13	0.5764
DIPE	HEX	1.30	314.29	−185.72	0.5726
Cl-HEX	MB	−0.06	384.74	−261.68	0.6480
MB	Cl-HEX	−0.68	371.82	−235.86	0.6918
HEX-Ac	MB	−0.29	557.17	−433.73	0.7141
MB	HEX-Ac	−1.21	373.03	−249.69	0.6918
DIPE	MB	−8.25	345.68	−232.58	0.5726
MB	DIPE	−6.42	348.10	−213.66	0.6918

MB mixtures, an outcome probably ascribable to the MB dipole moment (absent in HEX) that reinforces the solute−solvent interaction through an additional stronger contribution. The larger V_c values in MB mixtures bring about a large empty space and the solute−solvent interactions become increasingly unlikely; however, such an interaction is stronger compared to HEX mixtures, with lower V_c values. In sum, MB and HEX mixtures gave fairly similar partial molar solute volumes; that is, the geometry (more favorable in HEX mixtures) and interaction (more favorable in MB mixtures) contributions become balanced in their mixtures. It may then be concluded that the geometry effects arising from the molecular shape exert an effective control of the partial molar volume; likewise, remarkable interaction effects (more important in MB mixtures) have appeared, although not sufficient to neutralize the prevalent cavity formation expansion effect.

Thermophysical Properties of the Ternary Systems. Ternary mixtures are expected to show an even more complex behavior. The V_m^E values were negative over almost the full composition range except for DIPE mixtures (Figure 8), which were positive when $x_{MB} \rightarrow 0$. For Cl-HEX mixtures, the small ternary contribution to molar excess volumes (Figure 8d) was negative in the Cl-HEX-poor areas (8% at the minimum) and positive (23% at the maximum) in the rich ones (Table S6, Supporting Information); that is, ternary expansion effects appeared mainly in the Cl-HEX-rich region, although not sufficient to counteract the contraction term stemming from the binary contributions. The disruption of the dipolar ordering in pure MB and Cl-HEX, together with the rising distance among aliphatic chains on mixing, give rise to an small expansion contributionV_m^E. Likewise, the efficient packing concluded from analysis of the binary results contributes with the contraction term occasioned by pure geometry effects; the marked interaction among the permanent MB dipoles and Cl-HEX, though weak compared to pure components, contribute contracting the system. The maximum in the ternary contribution at low MB and high Cl-HEX contents bears a marked impact of the expansive ternary effects put down to the dilution of the Cl-HEX dipoles. For HEX-Ac mixtures, a contractive ternary contribution in HEX-rich areas, which amounts to 22% the property at that composition, and an expansion contribution in HEX-Ac rich-zones, which amounts to 12% the total property (Figure 8e), have appeared. Despite the disarray of the H-bonding structure, the prevalent negative ternary effects reveal that the efficient packing, made easier by the size and linear shape of the components, is even more remarkable when HEX dominates and determines the fluid structure. The modest expansive contribution at high HEX-Ac content (Table S6, Supporting Information) points to a marked disruption of the acid structure by addition of the remaining components, not compensated by the efficient molecular packing. For DIPE, a modest 9% contractive ternary contribution arose with a minimum at 1:1:2 HEX/DIPE/MB composition; thus, in a structure dominated by MB the ether fitting is best, and addition of MB favors the ether packing, as revealed by the negative molar excess volume compared to the positive values for HEX + DIPE mixture. The ether is prone to an efficient fitting in the MB structure due to the interaction of the dipoles, whereas addition of the almost globular ether to HEX brings about a remarkable disruption not balanced by new contractive contributions. That is, the molar excess volumes deduced point to a fluid structure primarily controlled by geometry effects (which favors an efficient interaction among components) with absence of marked ternary interactions.

The ternary mixing viscosities were negative over the full composition range for the three systems (Figure 9), indicating the prevalence of weak dispersive forces. For Cl-HEX, the small ternary contribution (Figure 9d and Table S6, Supporting Information) was positive over almost the full composition range with a 9% maximum in HEX-rich areas. The efficient packing of Cl-HEX and MB in HEX-dominated mixtures gives rise to a slight reinforcement of dipole−dipole interactions compared to those in binary systems and also to an increase of permanent-induced dipole forces, but in general the forces upon mixing become weakened compared to pure fluids. For HEX-Ac mixtures, the ternary contribution to mixing viscosity was negative over almost the full composition range with a 17% minimum at that composition. This contribution shows that the rupture of the H-bonding structure in HEX-Ac is the main controlling factor; the acid-MB H-bonding heteroassociation, if present, is weaker and does not balance the breaking of HEX-Ac dimers through H-bonding. The DIPE systems displayed positive ternary contributions with an 18% maximum; this feature denotes a certain extent of efficient ether-MB dipolar heteroassociation in the mixture, favored by the efficient ether packing in the MB structure. In view of the mixing viscosity data, involvement of strong ternary interactions should be ruled out; although heteroassociations are present in the mixtures to different extents depending on the components, the disruption of ordering in pure fluids prevails.

For the three studied systems, the predominantly positive mixing refractive indices confirm the above results (Figure 10); for Cl-HEX the negative contribution displayed a 80% miminum at that composition (Table S6, Supporting Information). Positive mixing refractive indexes can be originated by the raise in dipolar density inherent to the mixture contraction. The refractive index values increased compared to those of the pure components; the negative ternary contribution points to the marked effect arising from the dipole dilution and thus to a less efficient dipolar ordering compared to pure fluids. For HEX-Ac mixtures, the ternary contribution was positive over almost the full composition range with a 15% maximum at that composition; in principle, this contribution can point to the strong negative ternary contribution to molar excess volume. The prevailing negative ternary contribution to mixing viscosity leaves out strong heteroassociations that would produce a more positive contribution to ternary mixing refractive index. The DIPE mixtures showed a negative contribution to the mixing refractive index with a marked 133% minimum in ether-rich regions, where full fitting of the ester molecules ceases to be viable. The breakdown in the fluid structure introduced by the ether originates such a marked ternary effect, tending to lower the mixture refractive index, even though the dominating contractive factors give rise to a total positive mixing property.

The partial molar excess volumes $\bar{V}_m^E$ deduced for the ternary systems may lend an insight into the mixture structure.

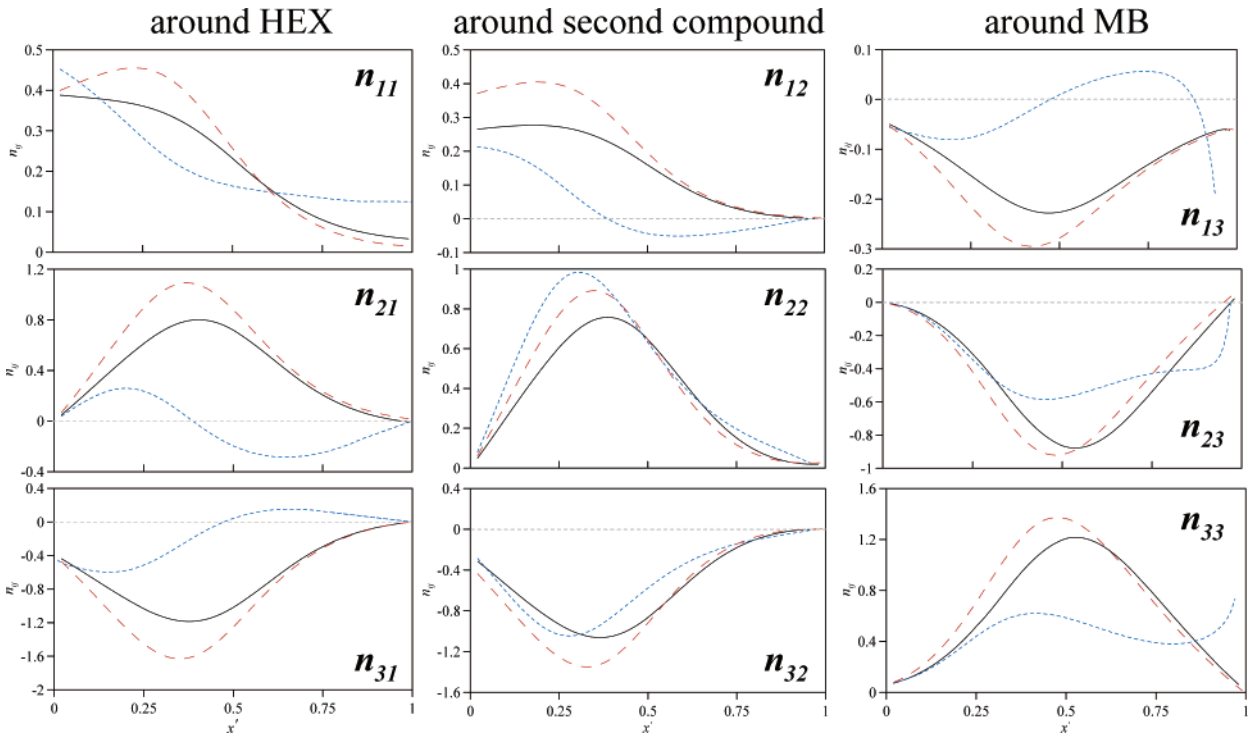

Figure 13. Excess of deficiency of molecules around a central one, $n_{ij,}$ in the pseudo-binary system x_1 HEX/x_2 Cl-HEX (or HEX-Ac or DIPE)/x_3 MB with constant $x_1 = 0.1$ calculated according to the KB theory at 298.15 K. $x' = x_2/(x_2 + x_3)$. 1 = HEX, 2 = Cl-HEX (or HEX-Ac or DIPE), 3 = MB. (—) Cl-HEX or (---) HEX-Ac or (— —) DIPE-containing ternary systems.

Figure 11 plots the MB partial molar volume of the three systems. The property with a complex behavior was negative for the three mixtures over almost the full composition range and shows the efficient MB fitting into the resulting fluid structure. The negative values also point to dipolar interactions that may favor a closer packing of the components but are insufficient to cancel out the order disruption in pure fluids. The very negative infinite dilution values (Figure 12) bear out such an effect and show that an effective MB solvation in all systems is feasible; the extremely negative values for DIPE mixtures can be ascribed to the efficient fitting of the globular MB molecules.

Kirkwood−Buff Analysis of Binary and Ternary Mixtures. Further information on the mixture structure may be inferred from KB analyses, also known as Fluctuation Theory. Preferential solvation, an effect that may act on the thermodynamic properties of mixtures, appears when the local composition in the solvation microsphere differs from that of the bulk one. This theory explores the linkage between the microscopic fluid structure and the macroscopic thermodynamic properties through an exact statistical mechanics model; such a linkage may be obtained through the so-called Kirkwood−Buff integrals (KBI), G_{ij}

$$G_{ij} = \int_0^\infty (g_{ij} - 1)4\pi r^2 dr \qquad (6)$$

where the g_{ij} stand for the radial distribution function of the species i around the central molecule j, and r is the distance between the centers of the two molecules. After the work by Ben−Naim,[17] calculation of KBIs requires the use of three macroscopic thermodynamic properties: isothermal compressibility, activity coefficients, and partial molar volumes. The partial molar volumes for ternary mixtures and their binary constituents are reported in this work. The isothermal compressibility contribution to G_{ij} is almost negligible,[44] and therefore they were regarded as ideal and determined from the literature values for pure components (Table 1). To properly determine the partial derivatives of the chemical potential required for the calculation of KBIs, the activity coefficients and their concentration dependence are needed. Unfortunately these were not experimentally available; therefore, we had to fall back on the Dortmund UNIFAC group contribution method.[45] The broad data basis used in this work to obtain the group parameters enables the model to provide reliable and accurate results; this approach has been used successfully for MB-containing systems.[15c,e] Matteoli[46] pointed out that if the KBIs of mixtures are examined to lend an insight into interactions and local composition then a suitable reference level must be established. The symmetrical ideal system can be regarded as a suitable reference level, that is, to get reliable information on the mixture structure the G_{ij}^{IDEAL} values for this reference level should be subtracted from the G_{ij} values. The G_{ij} values used in this work for the binary constituents and the ternary mixtures were obtained according to the above criteria from Ruckenstein et al.[44] Another crucial parameter, the excess (or deficit) number of molecules around a central one, n_{ij}, can be calculated from the G_{ij} values as

$$n_{ij} = c_i(G_{ij} - G_{ij}^{\mathrm{IDEAL}}) \qquad (7)$$

where c_i is the concentration of the i component. To simplify the analysis of mixed solvents behavior, the ternary mixtures were treated as pseudo binaries, that is, assuming constant mole fraction for one component and variable composition for the other two. Hence, each ternary system is split into three pseudo-binaries: x_1 (HEX) = 0.1, x_2 Cl-HEX (or HEX-Ac, or DIPE) = 0.1, and x_3 (MB) = 0.1 (Figure 1, Supporting Information). Results of KB analyses are shown in Figures 13−15.

The results for the pseudobinary x_1 (HEX) = 0.1 clearly point to like-solvation in the microspheres of all three components and the three studied systems (Figure 13). For these pseudobinaries with low HEX concentration, the high and positive n_{ii}

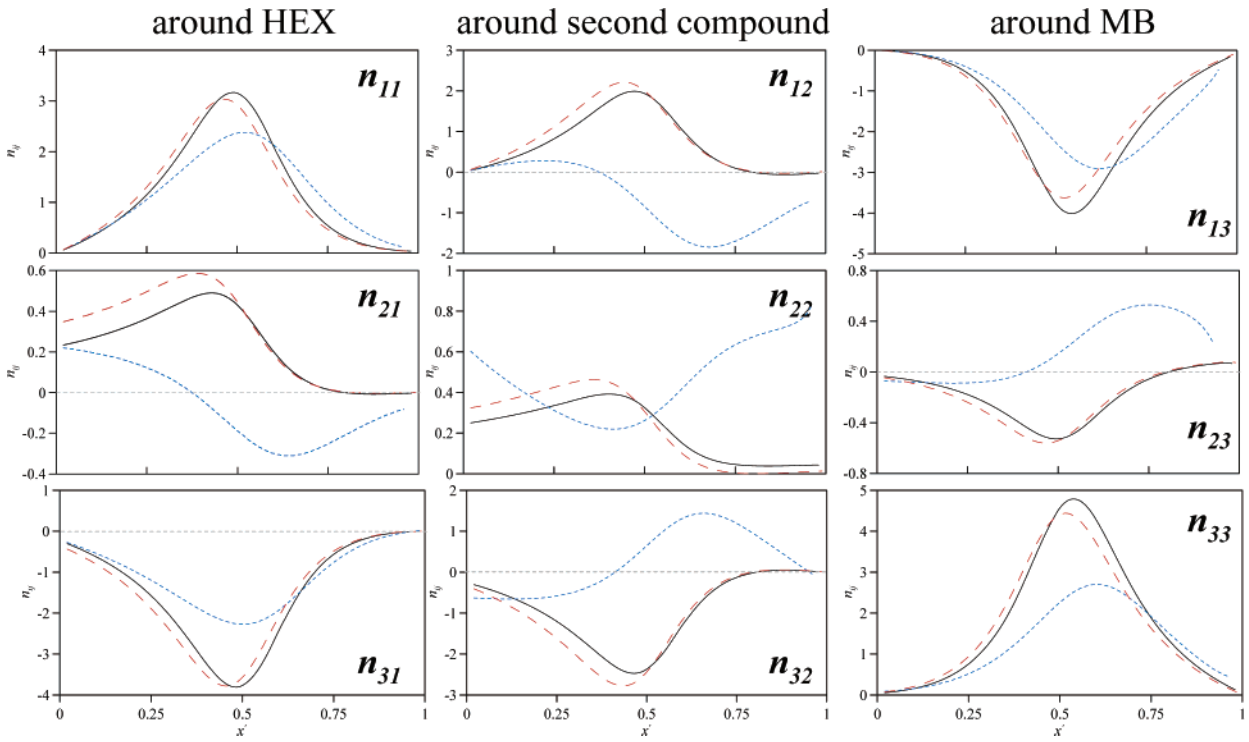

Figure 14. Excess of deficiency of molecules around a central one, $n_{ij,}$ in the pseudo-binary system x_1 HEX/x_2 Cl-HEX (or HEX-Ac or DIPE)/x_3 MB with constant $x_2 = 0.1$ calculated according to the KB theory at 298.15 K. $x' = x_1/(x_1 + x_3)$. Symbols and numbering as in Figure 13.

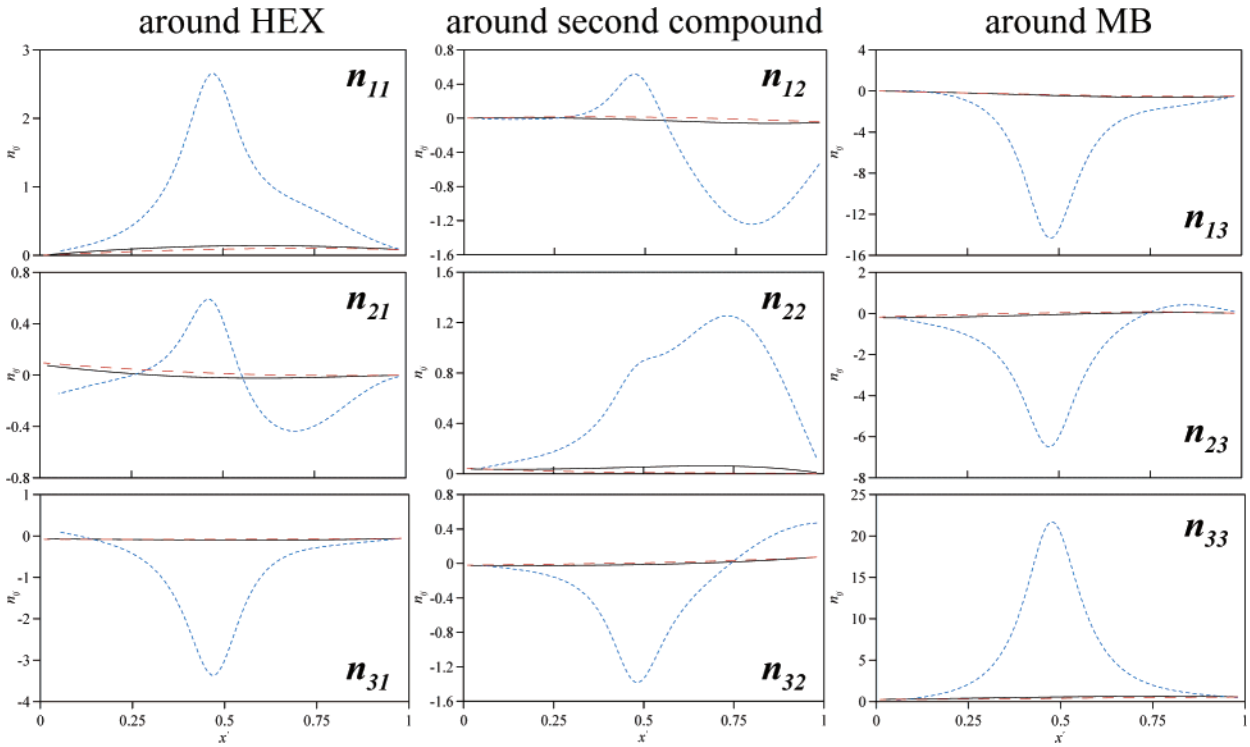

Figure 15. Excess of deficiency of molecules around a central one, $n_{ij,}$ in the pseudo-binary system x_1 HEX/x_2 Cl-HEX (or HEX-Ac or DIPE)/x_3 MB with constant $x_3 = 0.1$ calculated according to the KB Theory at 298.15 K. $x' = x_1/(x_1 + x_2)$. Symbols and numbering as in Figure 13.

functions deduced reveal like−like preferential solvation. The solvation sphere around HEX is dominated by HEX molecules; as the second component concentration is raised, mainly for Cl-HEX or DIPE, a notable amount of these molecules appear in the HEX solvation sphere. For HEX-Ac mixtures, at high acid concentration a deficit of this component may appear in the HEX microsphere due to its tendency to keep up the H-bonding structure. The striking DIPE excess in the HEX solvation sphere should be stressed here, a feature explained on the basis of the low HEX concentration. Conversely, there is an obvious MB deficit in the HEX microspheres, lower for the HEX-Ac mixture. This feature can be put down to the easier MB interaction with the acid compared to the ether or Cl-HEX mixtures; the MB planar shape seems to exclude this component from the HEX solvation sphere. A solvation analysis around the second component in the Cl-HEX (or HEX-Ac, or DIPE) mixtures reveals a behavior parallel to that around HEX, that is, the prevalence of like−like preferential solvation; such an

effect is even more remarkable for HEX-Ac mixtures due to its H-bonding ability with some HEX excess and MB deficit in the respective spheres. Around MB, the plots reflect that like−like solvation is more pronounced; the microspheres predominantly consist of MB molecules with a net deficit of the other components. Therefore, for this pseudobinary it is apparent the existence of microheterogeneities with the local composition differing from the bulk one.

Figure 14 summarizes the behavior of the second pseudo-binary, x_2 Cl-HEX (or HEX-Ac, or DIPE) = 0.1. The large n_{11} values suggest the prevalence of like−like solvation around HEX with a maximum at $x' = 0.5$. The positive n_{21} values denote a proper fitting of the Cl-HEX and DIPE molecules in the HEX microsphere. In contrast, the negative n_{21} values for HEX-Ac at high HEX concentrations indicate that HEX-Ac is turned away from the alkane microspheres at this acid concentration due to its H-bonding ability. Also, MB is turned away from the HEX microspheres and the more so as the alkane concentration increases (Figure 14). The solvation around Cl-HEX and DIPE differs sharply from that around HEX-Ac; the solvation spheres for the chloroalkane and ether mixtures consist of like and HEX molecules, whereas for the acid species the spheres consist of like and (only at high HEX concentration) MB molecules. That is, when the HEX concentration is raised some molecules are forced to pass to the acid microspheres. Furthermore, the behavior around MB reveals like−like preferential solvation; this trend is altered only for the HEX-Ac system as the HEX content rises, a region where some acid molecules are included in the ester microspheres. According to these results, the behavior of the acid-containing system differs from that of the other mixtures; a boost in the HEX content brings about mixed MB-acid solvation spheres, where both molecules interact probably through dipolar interactions. At low concentration, the acid is prone to keep up the excess in the HEX spheres, but at high concentration it is impelled by the alkane to the bulk solvent, where interaction with the MB microspheres comes about. This feature was not observed for Cl-HEX and DIPE, which are more efficiently packed in the HEX microspheres; if the alkane concentration is high enough, then the amount for the former components drop.

The behavior of the pseudo-binary x_3 (MB) = 0.1 (Figure 15) differs sharply. Although like−like preferential solvation prevails, the HEX-Ac system behaves differently; at this specific low ester concentration, a soft like−like solvation around HEX prevails for Cl-HEX and DIPE, but it becomes quite pronounced for HEX-Ac even though the acid is also present at low alkane concentration. Absence of MB in the HEX solvation sphere is evident. The like−like structure around HEX-Ac also prevails, although the presence of modest amounts of HEX molecules at high acid concentration and of MB at high alkane concentration should be noticed. Finally, the MB solvation sphere consists of MB molecules. At such low MB concentrations, MB is surrounded by like molecules on an almost exclusive basis, and only in the HEX-rich region are some acid molecules able to enter in the ester microspheres.

In summary, the KB analysis carried out points to the existence of microheterogeneities in the fluid structure for all the studied systems with the local composition clearly differing from the bulk one. HEX, Cl-HEX, and DIPE tend to form mixed solvation spheres, whereas HEX-Ac and MB show a closer reciprocal affinity and may be found in the corresponding solvation surroundings. To account for such an acid-ester affinity, the energy and structure of the gas-phase MB/(Cl-HEX or HEX-Ac or DIPE) pairs have been determined at B3LYP/6-311++g** theoretical level (Figure 16). From the calculated complex structure, it is clear that MB and HEX-Ac may form stable gas-phase H-bonds. In liquid mixture, it stands to reason that such bonds, hindered by like molecules in the solvation sphere of both components, account for the mutual affinity as well as the marked presence in the respective solvation spheres; in sharp contrast is the observed trend for Cl-HEX and DIPE systems, for which only a low affinity between both molecules may be inferred (Figure 16). Although the acid-ester H-bonding should be either left out or considered much weaker than in gas phase, a marked affinity between both components is established, giving rise to noticeable dispersive or dipolar interactions. The remaining components are prone to forming heterogeneous solvation spheres among them, probably because their size and shape are quite similar; even the almost globular DIPE is able to enter in the solvation sphere of the linear alkane. This effect, appearing mainly at low alkane or low ether concentrations, comes about despite the steric hindrance inherent to introducing globular ether molecules into the alkane one.

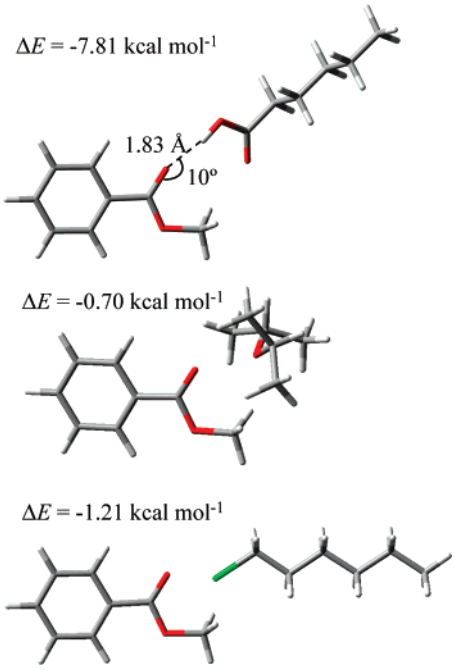

Figure 16. Gas-phase structure of MB/(HEX-Ac or DIPE or Cl-HEX) complexes calculated at B3LYP/6-311++g** theoretical level. Values indicate binding energy, ΔE, hydrogen-bonding distance, and angle (for HEX-Ac). Color code as in Figure 1.

Modeling of Thermophysical Ternary Properties. *Semiempirical Models.* Prediction of multicomponent systems from available properties of the binary constituents is quite a useful task considering the scarcity of these properties and the difficulty of their experimental determination. An approach of broad appeal consists of using semiempirical models. Despite the absence of a deep theoretical basis, these may enable one to obtain reliable results mainly in systems where ternary interactions are unimportant.[18] These models may be classified as either asymmetric, if they are dependent on the arbitrary numbering of the mixture components, or symmetric. The symmetric models by Jacob−Fitzner, Köhler, and Colinet, together with the asymmetric by Tsao−Smith, Toop, and Scatchard, were tested; the prediction for molar excess volume, mixing viscosity, and mixing refractive index are reported in Table 3. The main features of these models[18] and their applications were described in detail.[15c,e] The quality of predictions obtained with the simple symmetric models was high for all the studied properties and

TABLE 3: Standard Deviation, σ, for the Predictions Obtained with Semiempirical Models for the x_1 HEX + x_2 Cl-HEX (or HEX-Ac, or DIPE) + $(1 - x_1 - x_2)$ MB Ternary System at 298.15 K

model	σ ($\sigma V^E_{m,TER}$) (cm^3 mol^{-1})			σ ($\Delta_{mix}\eta_{TER}$) (mPa s)			σ ($\Delta_{mix}n_{D,TER}$)		
				x_1 HEX + x_2 Cl-HEX + $(1 - x_1 - x_2)$ MB					
Jacob-Fitzner		0.0413			0.015			0.0010	
Köhler		0.0443			0.017			0.0010	
Colinet		0.0442			0.015			0.0010	
Tsao-Smith	0.0457[a]	0.0895[b]	0.0505[c]	0.064[a]	0.078[b]	0.007[c]	0.0010[a]	0.0019[b]	0.0010[c]
Toop	0.0409[a]	0.0486[b]	0.0563[c]	0.032[a]	0.018[b]	0.010[c]	0.0012[a]	0.0011[b]	0.0009[c]
Scatchard	0.0419[a]	0.0486[b]	0.0521[c]	0.032[a]	0.017[b]	0.011[c]	0.0012[a]	0.0011[b]	0.0009
				x_1 HEX + x_2 HEX-Ac + $(1 - x_1 - x_2)$ MB					
Jacob-Fitzner		0.0571			0.058			0.0007	
Köhler		0.0627			0.049			0.0007	
Colinet		0.0621			0.051			0.0007	
Tsao-Smith	0.0346[a]	0.0837[b]	0.0678[c]	0.036[a]	0.028[b]	0.080[c]	0.0006[a]	0.0010[b]	0.0008[c]
Toop	0.0419[a]	0.0680[b]	0.0811[c]	0.029[a]	0.081[b]	0.071[c]	0.0006[a]	0.0007[b]	0.0010[c]
Scatchard	0.0439[a]	0.0671[b]	0.0751[c]	0.028[a]	0.084[b]	0.079[c]	0.0006[a]	0.0007[b]	0.0010[c]
				x_1 HEX + x_2 DIPE + $(1 - x_1 - x_2)$ MB					
Jacob-Fitzner		0.0675			0.022			0.0045	
Köhler		0.0669			0.023			0.0049	
Colinet		0.0670			0.022			0.0046	
Tsao-Smith	0.2040[a]	0.0496[b]	0.1103[c]	0.084[a]	0.088[b]	0.009[c]	0.0071[a]	0.0040[b]	0.0060[c]
Toop	0.0550[a]	0.0833[b]	0.0660[c]	0.038[a]	0.027[b]	0.009[c]	0.0051[a]	0.0033[b]	0.0060[c]
Scatchard	0.0533[a]	0.0851[b]	0.0653[c]	0.039[a]	0.025[b]	0.009[c]	0.0047[a]	0.0033[b]	0.0060[c]

[a] For asymmetric equations, the component 1 is HEX. [b] For asymmetric equations, the component 1 is Cl-HEX (or HEX-Ac or DIPE). [c] For asymmetric equations, the component 1 is MB.

systems and comparable to those obtained with the more complex asymmetric ones. To attain lowest deviations with asymmetric models, numbering as one the common component of the two binary constituents with greater deviations from ideality (or from mixing property equals zero) is highly recommended;[47] this criterion led to lower deviations for the three asymmetric models tested (Table 3). Absence of strong ternary interactions in the studied systems yielded low deviations with any of the models tested.

Cubic EOS. The correlation and/or prediction of molar excess volumes rely on the choice of a suitable EOS combined with the proper mixing rule. Despite their theoretical and computational simplicity, the cubic EOS by Soave (SRK)[19] and Peng−Robinson (PR)[20] often used to determine volumetric properties of multicomponent mixtures have provided good results even with mixtures of polar solvents such as those in this work. Both EOS were used combined with a simple one-parameter van der Waals type mixing rule for which only a single binary interaction parameter, k_{12}, is required. This parameter was obtained from correlation of experimental molar excess volumes of the binary constituents and used to predict the ternary systems, that is, the ternary effects were disregarded.[15c,e] Thus, this approach may be considered as correlative for binaries and predictive for higher order mixtures. Table 4 lists the results of the EOS study. Low deviations were obtained in the correlation of molar excess volumes for the binary constituents. Both equations of state gave similar results, and only the deviations for the HEX + HEX-Ac binary system were too high. Bearing in mind the one-parameter nature of the mixing rule, the predictive ability of these equations was rather good, and only the system containing HEX-Ac gave greater deviations. Therefore, cubic EOS can be applied for the correlation and prediction of molar excess volumes in aromatic ester-containing binary mixtures. Despite the simplicity of the models used, the parameters obtained may afford high-quality predictions in multicomponent mixtures; improving the predictions in systems with higher affinity with molecules such as HEX-Ac probably requires a more complex mixing rule.

TABLE 4: k_{12} and m_{12} Parameters and Standard Deviations, σ, Deduced from Application of Soave (SRK) and Peng−Robinson (PR) Cubic EOS with a One-Parameter van der Waals Mixing Rule for Molar Excess Volume (cm^3 mol^{-1}) Correlation (binary Systems) and Prediction (Ternary Systems) at 298.15 K

	SRK		PR	
mixture	k_{12}	σ (cm^3 mol^{-1})	k_{12}	σ (cm^3 mol^{-1})
HEX + Cl-HEX	0.0674	0.0392	0.0634	0.0247
HEX + HEX-Ac	0.1847	0.2866	0.1727	0.2166
HEX + DIPE	0.0181	0.0183	0.0206	0.0184
HEX + MB	0.0944	0.0379	0.0939	0.0375
Cl-HEX + MB	0.0001	0.0226	−0.0015	0.0231
HEX-Ac + MB	−0.0129	0.0204	−0.0174	0.0204
DIPE + MB	0.0162	0.0570	−0.0083	0.0925
HEX + Cl-HEX + MB		0.0680		0.0589
HEX + HEX-Ac + MB		0.1626		0.1222
HEX + DIPE + MB		0.0492		0.0765

Concluding Remarks

On the basis of the measured thermophysical properties and the theoretical models applied, the analysis performed on the MB ternary mixtures points to complex structures. At a molecular level, like−like preferential solvation is deduced by KB analyses for all ternary systems. Even though the HEX-Ac mixture is characterized by the presence in the acid and ester solvation spheres of both molecules, this fact points to a great affinity between molecules. Conversely, for Cl-HEX and DIPE mixtures only HEX is also present in their solvation spheres, whereas MB is left out; this feature can be justified by geometry effects. The reported thermophysical properties point to weakening and disruption of intermolecular forces upon mixing and the prevalence of steric effects that give rise to efficient packing in most mixtures. The analysis of properties through semiem-

pirical models and simple cubic EOS yielded satisfactory results that have enabled us to rule out the existence of noticeable ternary effects; only the HEX-Ac mixture gave worse predictions, which points to a more structured fluid whose properties are only poorly described by the simple models.

Acknowledgment. The financial support by Junta de Castilla y León, Project BU-020A/07, and Ministerio de Educación y Ciencia, Project CTQ2005-06611/PPQ, (Spain) are gratefully acknowledged.

Supporting Information Available: Table S1 (properties of pure solvents), Table S2 (binary systems data), Table S3 (ternary systems data), Table S4 (Redlich−Kister coefficients), Table S5 (Cibulka coefficients), Table S6 (extremes of ternary contributions), and Figure 1 (Scheme of pseudo-binary mixtures for Kirkwood−Buff analysis). This material is available free of charge via the Internet at http://pubs.acs.org.

References and Notes

(1) Archer, W. L. *Industrial solvents handbook*; Marcel Dekker: New York, 1996.
(2) Marcus, Y. *Solvent mixtures. Properties and selective solvation*; Marcel Dekker: New York, 2002.
(3) Chen, C. C.; Mathias, P. M. *AIChE J.* **2002**, *48*, 194.
(4) Dohrn, R.; Pfohl, O. *Fluid Phase Equilib.* **2002**, *194*−*197*, 15.
(5) Harvey, A. H.; Laesecke, A. *Chem. Eng. Prog.* **2002**, *98*, 34.
(6) Rainwater, J. C.; Friend, D. G.; Hanley, H. J. M.; Harvey, A. H.; Holcomb, C. D.; Laesecke, A.; Magee, J. W.; Muzny, C. *J. Chem. Eng. Data* **2001**, *45*, 1002.
(7) Raal, J. D.; Muhlbauer, A. L. *Phase equilibria. Measurement and computation*; Taylor and Francis: London, 1998.
(8) Prausnitz, J. M.; Lichtenthaler, R. M.; Gomes de Azevedo, E. *Molecular thermodynamics of fluid phase equilibria*; Prentice Hall: New York, 1998.
(9) Deem, M. W. *AIChE J.* **1998**, *44*, 2569.
(10) Rhodes, C. L. *J. Chem. Eng. Data* **1996**, *41*, 947.
(11) Cipra, B. *Science* **2000**, *287*, 960.
(12) Zielkiewicz, J. *Phys. Chem. Chem. Phys.* **2000**, *2*, 2925.
(13) Kirkwood, J. G.; Buff, F. P. *J. Chem. Phys.* **1951**, *19*, 774.
(14) (a) Tsierkezos, N. G.; Kelarakis, A. E.; Molinou, I. E. *J. Chem. Eng. Data* **2000**, *45*, 776. (b) Semeniuk, B.; Wilczura-Wachnick, H. *Fluid Phase Equilib.* **1998**, *152*, 337. (c) Ortega, J.; Postigo, M. A. *Fluid Phase Equilib.* **1995**, *108*, 121. (d) García, B.; Ortega, J. C. *J. Chem. Eng. Data*. **1988**, *33*, 200. (e) García, B.; Ortega, J. C. *Thermochim. Acta* **1987**, *117*, 219. (f) Aminabhavi, T. M.; Raikar, S. K. *Collect. Czech. Chem.Commun*. **1993**, *58*, 1761. (g) Aminabhavi, T. M.; Phayde, H. T. S.; Khinnavar, R. S.; Gopalakrishna, B. *J. Chem. Eng. Data* **1994**, *39*, 251. (h) Dusart, O.; Piekarski, C.; Piekarski, S.; Viallard, A. *J. Chim. Phys*. **1976**, *78*, 837. (i) Grolier, J. P. E.; Ballet, D.; Viallard, A. *J. Chem. Thermodyn*. **1974**, *6*, 895.
(15) (a) García, B.; Alcalde, R.; Aparicio, S.; Leal, J. M. *Ind. Eng. Chem. Res.* **2002**, *41*, 4399. (b) García, B.; Alcalde, R.; Aparicio, S.; Leal, J. M. *Phys. Chem. Chem. Phys.* **2002**, *4*, 5833. (c) García, B.; Aparicio, S.; Alcalde, R.; Leal, J. M. *J. Phys. Chem. B* **2003**, *107*, 13478. (d) García, B.; Aparicio, S.; Navarro, A. M.; Alcalde, R.; Leal, J. M. *J. Phys. Chem. B* **2004**, *108*, 15841. (e) Aparicio, S.; Alcalde, R.; Leal, J. M.; García, B. *J. Phys. Chem. B* **2005**, *109*, 6375. (f) Aparicio, S.; Alcalde, R.; García, B.; Leal, J. M. *Ind. Eng. Chem. Res.* **2005**, *44*, 7575. (g) Alcalde, R.; Aparicio, S.; García, B.; Leal, J. M. *J. Phys. Chem. B* **2005**, *109*, 19908.
(16) Pierotti, R. A. *Chem. Rev.* **1976**, *76*, 717.
(17) Ben−Naim, A. *J. Chem. Phys*. **1977**, *67*, 4884.
(18) Acree, W. E. *Thermodynamic properties of nonelectrolyte solutions*; Academic Press: New York, 1984.
(19) Soave, G. *Chem. Eng. Sci*. **1972**, *27*, 1197.
(20) Peng, Y.; Robinson, D. B. *Ind. Eng. Chem. Fundam.* **1976**, *15*, 59.
(21) Valderrama, J. O. *Ind. Eng. Chem. Res*. **2003**, *42*, 1603.
(22) Riddick, J. A.; Bunger, W. B.; Sakano, T. K. *Organic solvents*; Wiley: New York, 1986.
(23) Dymond, J. H.; Oye, H. A. *J. Phys. Chem. Ref. Data* **1994**, *23*, 41.
(24) Santana, P.; Balseiro, J.; Salgado, J.; Jiménez, E.; Legido, J. L.; Carballo, E.; Andrade, M. I. P. *J. Chem. Eng. Data* **1999**, *44*, 1195.
(25) Petrino, P. J.; Gaston, Y. H.; Chevalier, J. L. E. *J. Chem. Eng. Data* **1995**, *40*, 136.
(26) Alcalde, R.; Aparicio, S.; García, B.; Dávila, M. J.; Leal, J. M. *New. J. Chem.* **2005**, *29*, 817.
(27) http://webbook.nist.gov/chemistry/ (accessed January 20, 2007).
(28) Becke, A. D. *Phys. Rev. A* **1988**, *38*, 3098.
(29) Lee, C.; Yang, W.; Parr, R. G. *Phys. Rev. B* **1988**, *37*, 785.
(30) Becke, A. D. *J. Chem. Phys.* **1993**, *98*, 5648.
(31) Singh, U. C.; Kollman, P. A. *J. Comput. Chem.* **1984**, *5*, 129.
(32) Besler, B. H.; Merz, K. M.; Kollman, P. A. *J. Comput. Chem*. **1990**, *11*, 431.
(33) Frisch, M. J.; Trucks, G. W.; Schlegel, H. B.; Scuseria, G. E.; Robb, M. A.; Cheeseman, J. R.; Montgomery, J. A., Jr.; Vreven, T.; Kudin, K. N.; Burant, J. C.; Millam, J. M.; Iyengar, S. S.; Tomasi, J.; Barone, V.; Mennucci, B.; Cossi, M.; Scalmani, G.; Rega, N.; Petersson, G. A.; Nakatsuji, H.; Hada, M.; Ehara, M.; Toyota, K.; Fukuda, R.; Hasegawa, J.; Ishida, M.; Nakajima, T.; Honda, Y.; Kitao, O.; Nakai, H.; Klene, M.; Li, X.; Knox, J. E.; Hratchian, H. P.; Cross, J. B.; Adamo, C.; Jaramillo, J.; Gomperts, R.; Stratmann, R. E.; Yazyev, O.; Austin, A. J.; Cammi, R.; Pomelli, C.; Ochterski, J. W.; Ayala, P. Y.; Morokuma, K.; Voth, G. A.; Salvador, P.; Dannenberg, J. J.; Zakrzewski, V. G.; Dapprich, S.; Daniels, A. D.; Strain, M. C.; Farkas, O.; Malick, D. K.; Rabuck, A. D.; Raghavachari, K.; Foresman, J. B.; Ortiz, J. V.; Cui, Q.; Baboul, A. G.; Clifford, S.; Cioslowski, J.; Stefanov, B. B.; Liu, G.; Liashenko, A.; Piskorz, P.; Komaromi, I.; Martin, R. L.; Fox, D. J.; Keith, T.; Al-Laham, M. A.; Peng, C. Y.; Nanayakkara, A.; Challacombe, M.; Gill, P. M. W.; Johnson, B.; Chen, W.; Wong, M. W.; Gonzalez, C.; Pople, J. A. *Gaussian 03*, revision C.02; Gaussian, Inc.: Wallingford, CT, 2004.
(34) Scaife, W. G. *Ber. Bunsen-Ges. Phys. Chem*. **1990**, *94*, 78.
(35) Redlich, T. A.; Kister, O. *Ind. Eng. Chem*. **1948**, *40*, 345.
(36) Cibulka, I. *Collect. Czech. Chem. Commun.* **1982**, *47*, 1414.
(37) (a) Mognaschi, E. R.; Chierico, A. *Z. Naturforsch.* **1986**, *41*, 491. (b) Mognaschi, E. R.; Zullino, L.; Chierico, A. *J. Phys. D. Appl. Phys*. **1984**, *17*, 1007. (c) Mognaschi, E. R.; Laboranti, L. M.; Chierico, A. *J. Phys. II* **1993**, *3*, 1271.
(38) Pico, J. M.; Menaut, C. P.; Jiménez, E.; Legido, J. L.; Fernández, J.; Andrade, M. I. P. *J. Chem. Soc., Faraday Trans.* **1996**, *92*, 4453.
(39) Vong, W. T.; Say, F. N. *J. Chem. Eng. Data* **1997**, *42*, 1116.
(40) Peng, D. Y.; Benson, G. C.; Lu, B. C. *J. Sol. Chem*. **1999**, *28*, 505.
(41) Pecar, D.; Dolecek, V. *Fluid Phase Equilib.* **2003**, *211*, 109.
(42) Lepori, L.; Gianni, P. *J. Sol. Chem*. **2000**, *29*, 405.
(43) Majer, V.; Svoboda, V. *Enthalpies of vaporization of organic compounds*; Blackwell Scientific Publications: Cambridge, MA, 1985.
(44) Ruckenstein, E.; Shulgin, I. *Fluid Phase Equilib.* **2001**, *180*, 281.
(45) Gmehling, J.; Li, J.; Schiller, M. *Ind. Eng. Chem. Res.* **1993**, *32*, 178.
(46) Matteoli, E. *J. Phys. Chem. B*. **1997**, *101*, 9800.
(47) Pando, C.; Renuncio, J. A. R.; Calzón, J. A. G.; Christensen, J. J.; Izatt, R. M. *J. Sol. Chem*. **1987**, *16*, 503.